Article ID: 1003－6326(2003)04－0830－05

Theoretical analysis of bubble nucleation in GASAR materials①

LIU Yuan(刘 源), LI Yanxiang(李言祥)
(Department of Mechanical Engineering, Tsinghua University, Beijing 100084, China)

Abstract: Nucleation of gaseous hydrogen bubbles is the initial stage of GASAR process. Through the theoretical analysis, it has been identified that heterogeneous nucleation of bubbles as caps on the solid surfaces of impurities is impossible and only the heterogeneous nucleation in pits and cracks in impurities is the most feasible way in the GASAR process. The results also show that the probability of bubble nucleation progressively decreases from Al, Cu and Ni to Fe molten metal, which is the result of the increasing adhesion work of liquid metal on alumina.

Key words: GASAR; porous metal; bubble nucleation
CLC number: TG 146.4 **Document code:** A

1 INTRODUCTION

Porous materials can be produced by using a novel method called GASAR developed in the Dnepropetrovsk Metallurgical Institute (DMI) of Ukraine[1]. Most metal-hydrogen binary systems have a eutectic decomposition similar to the classical eutectic system. These metals can be melted, saturated with hydrogen, and then directionally solidified, as shown in Fig. 1[2]. The porosity of the solidified GASAR materials can be varied through process variables such as pressure, rate and direction of cooling in a process based on gas-solid eutectic solidification[1].

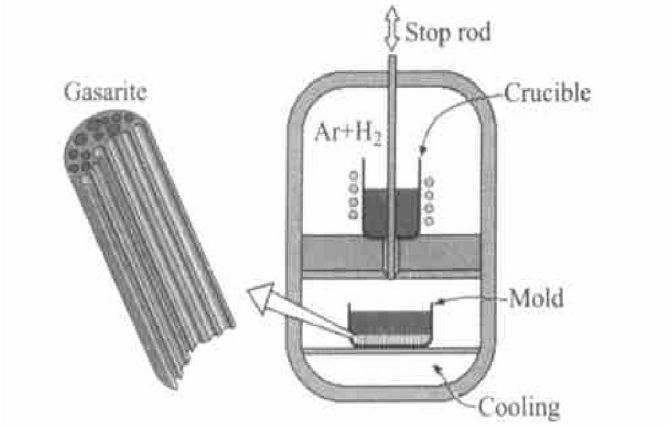

Fig. 1 Experimental GASAR apparatus and obtained Gasarite structure[2]

Materials that have been processed through GASAR technique include metals (Cu, Ni, bronze, Mg, Al, steel), alumina-magnesia ceramics, and glasses. The pores in GASAR materials may be continuous or discontinuous and can be manipulated to suit the needs for application. To achieve properly controlled porosity, however, it is important to understand the nucleation mechanism of the pores and control the governing parameters.

In the GASAR process, high hydrogen pressures are applied to saturate the melt, then partly or totally released to nucleate gaseous pores. Calculations[3] showed that unrealistically high pressures were needed to get appreciable homogeneous nucleation in the melt or heterogeneous nucleation at the solidification front. A critical investigation is thus needed to find a realistic mechanism for nucleation in order to explain the fact that the GASAR process does indeed produce many pores. The present work investigates different ways to heterogeneously nucleate pores as gaseous bubbles.

2 NUCLEATION OF GASEOUS PORES

The thermodynamic limit for the nucleation of pores as gaseous bubbles is determined by the maximum solubility, viz saturation limit of H in the metal. The dependence of the saturation limit on the hydrogen pressure and concentration is illustrated in Fig. 2—the phase diagram of Metal-Hydrogen system. At temperature and concentrations in $l+g$ or $l+s$ regions the dissolved hydrogen in the metal becomes unstable and is no longer in equilibrium with the dissolved hydrogen, which causes hydrogen bubbles to form. The nucleation of bubbles may occur in the liquid melt, in the solidified region, or in the solidification front. The latter case is suitable from a GASAR processing point of view since it allows the pores to grow alongside the solid front and form eutectic-like structures.

① **Foundation item:** Project(20020003086) support by the Doctoral Foundation and Post-Doctoral Foundation of China
Received date: 2002－12－31; **Accepted date:** 2003－04－19
Correspondence: LIU Yuan, PhD; Tel: +86-10-62773640; Fax: +86-10-62773637; E-mail: yuanliu@mail.tsinghua.edu.cn

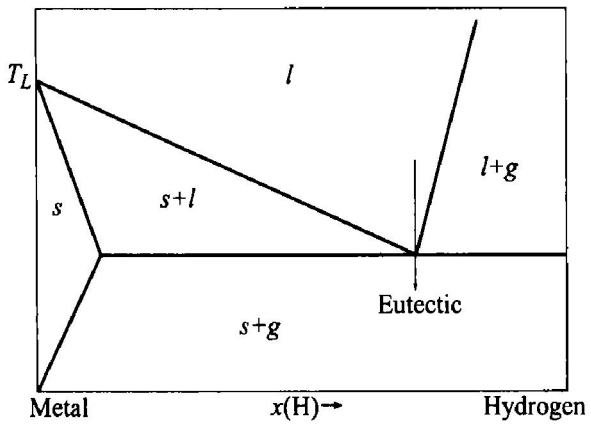

Fig. 2 Schematic phase diagram of metal-hydrogen

2.1 Homogeneous bubble nucleation

The change in free energy to form a spherical bubble of radius r in a liquid is

$$\Delta G = 4\pi r^2 \sigma_{lg} - \frac{4}{3}\pi r^3 \Delta p \quad (1)$$

where σ_{lg} is the liquid-gas interfacial energy, Δp is the pressure difference between the pressure inside the bubble (p_b) and the pressure in the liquid in the vicinity of the bubble (p). The second term on the right side represents the difference between a positive contribution to the free energy due to the work expended against the pressure in the liquid to form the bubble, and a negative contribution to the free energy due to allowing the bubble to fill with gas at a pressure p_b. The corresponding free energy to form a critical radius is therefore

$$\Delta G_c = 16\pi\sigma_{lg}/3(\Delta p)^2 \quad (2)$$

The nucleation rate can be expressed as[4]

$$J = \frac{NkT}{h}\exp\left|\frac{-(\Delta G_d + \Delta G_c)}{kT}\right| \quad (3)$$

where J is the number of nuclei formed per mole of liquid, ΔG_d is the free energy of activation for diffusion in the liquid, T is the temperature in K, and N, k, h are Avagadro's number, Boltzmann's constant, and Planck's constant, respectively.

The pre-exponential factors in Eq. (3) are so small that appreciable nucleation occurs only if $\Delta G_c/kT < 60$[4]. Many metals including Cu, Ni, bronze, Mg, Al, steel, Mg have the minimum interfacial energies in which $\sigma_{lg} \approx 0.56$ J/m^2[5]. For Mg, $\Delta G_c/kT < 60$ and $T > 922$ K would correspond to a Δp of more than 1.96 GPa. This pressure difference is far too high from a process point of view, where the pressure difference are likely to be several orders of magnitude lower in GASAR processing[6-9]. So homogeneous nucleation of bubbles does not occur in the GASAR process of Mg. For the other metals, the homogeneous nucleation of bubbles also can not occur due to their higher interfacial energies than Mg.

2.2 Heterogeneous bubble nucleation

Hydrogen pressures in the GASAR process are typically between 0.1 and 1 MPa. Homogeneous bubble nucleation is easily shown to be impossible. There is ample experimental evidence that shows bubble nucleation occurs heterogeneously on partially-wetted inclusions[9-14]. Most molten metals contain oxide which may be engulfed or rejected by the moving solid-liquid interface. Impurities such as the ceramic oxides Al_2O_3 and SiO_2 may act as favorable sites for heterogeneous nucleation of gas pores.

2.2.1 Bubble nucleation on planar interfaces

In the simplest case bubbles would nucleate as spherical caps under the geometric conditions shown in Fig. 3. The free energy for the cap-formed bubble as it grows will include two negative contributions representing the pressure difference and the decrease in the solid-liquid surface energy. The positive contributions include terms for the increase in the liquid-gas and solid-gas surface. The activation energy is given by

$$\Delta G_c = [16\pi\sigma_{lg}^3/3(\Delta p)^2] \cdot f(\theta_c) \quad (4a)$$

$$f(\theta_c) = (2 - 3\cos\theta_c + \cos^3\theta_c)/4 \quad (4b)$$

where θ_c is the contact angle of the bubble on the solid. The contact angle is determined by the balance of the three surface energies involved.

$$\cos\theta_c = 1 - W/\sigma_{lg} \quad (5a)$$

$$W = \sigma_{sg} + \sigma_{lg} - \sigma_{ls} \quad (5b)$$

where W is referred to as the adhesion work and represents the degree of wetting of the liquid on the solid. It is evident from equations (4) and (5) that the nucleation process is favored on solid surfaces on which the liquid melt has a small θ_c, or equivalently a very small adhesion work. Table 1 lists the required Δp for hydrogen bubble nucleation on the surface of Al_2O_3 inclusion in different metals. It is obvious that the required Δp for hydrogen bubble nucleation on the surface of Al_2O_3 inclusion are all in the order of GPa, which indicates that the heterogeneous nucleation on a planar liquid metal: solid ceramic interface thus will not occur under the conditions of GASAR processing. In addition, Δp increases with the rise of the adhesion work(W), which indicates that the heterogeneous nucleation becomes more and more difficult with increasing W.

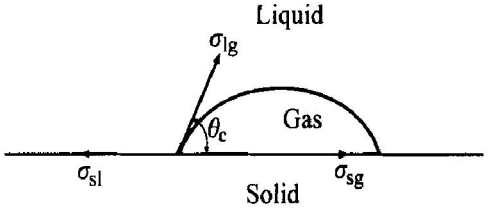

Fig. 3 Gaseous bubbles growing as spherical caps on solid surface

Table 1 Required Δp for hydrogen bubble nucleation on surface of Al_2O_3 inclusion in different metals (degree of superheat is 100 K)

Metal	Al			Cu			Ni			Fe		
Parameter	W/ (Jm^{-2})	σ_{lg}/ (Jm^{-2})	θ_c/ (°)	W/ (Jm^{-2})	σ_{lg}/ (Jm^{-2})	θ_c/ (°)	W/ (Jm^{-2})	σ_{lg}/ (Jm^{-2})	θ_c/ (°)	W/ (Jm^{-2})	σ_{lg}/ (Jm^{-2})	θ_c/ (°)
	0.25	0.85	135	0.40	1.30	134	0.638	1.66	128	1.211	1.84	110
Δp/GPa	0.835			1.384			2.274			4.202		

σ_{lg} and θ_c come from Ref. [15] and W is obtained from $W=\sigma_{lg}(1-\cos\theta_c)$.

The solidification front itself also can be a site for heterogeneous nucleation. But for the interface between a solid metal and its melt, W will be several Joules per square meter, which rules out bubble nucleation there.

2.2.2 Bubble nucleation in pits and cracks

Table 1 shows that nucleation on a flat impurity surface is unlikely. Tiwari and Beech[11] observed the aluminum oxide inclusions on polished Al alloy samples using optical and scanning electron microscopy and found that these aluminum oxide particles 5 to 300 μm in size contained pores and cracks on the order of 1 to 40 μm. It is obvious that the heterogeneous nucleation on the impurities will be easier if pits or cracks are present on the solid surface.

In the case that the pit is conical, the gas phase will grow in the geometry shown in Fig. 4. For mathematical simplicity the growing pores are assumed to have an interface with the liquid that is approximately flat. It should be noted that this is not the case in the nearest vicinity of the solid where the liquid will have some degree of wetting. The relative error introduced is expected to be small. The free energy in this case is

$$\Delta G=-\Delta p\,\pi r^3/3\tan(\alpha/2)+(\sigma_{sg}-\sigma_{ls})\pi r^2/\sin(\alpha/2)+\pi r^2\sigma_{lg} \quad (6)$$

The corresponding free energy to form a critical radius of the conical cavity required for nucleation is calculated from Eq. (7):

$$\Delta G_c=\frac{4}{3}\pi\frac{[W+\sigma_{lg}(\sin(\alpha/2)-1)]^3}{\sin(\alpha/2)\cdot[\Delta p\cos(\alpha/2)]^2} \quad (7)$$

Fig. 5 plots the critical nucleation energy vs the apex angles of the conical cavity for physically reasonable material and processing parameters and

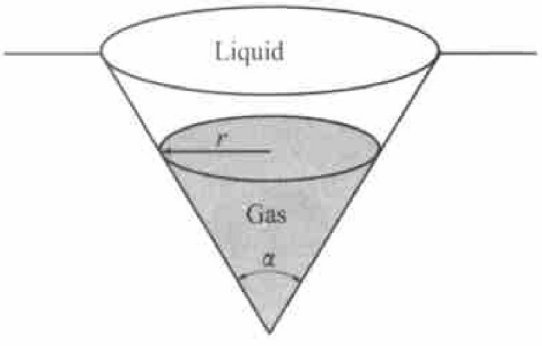

Fig. 4 Gaseous bubble growing in conical pit

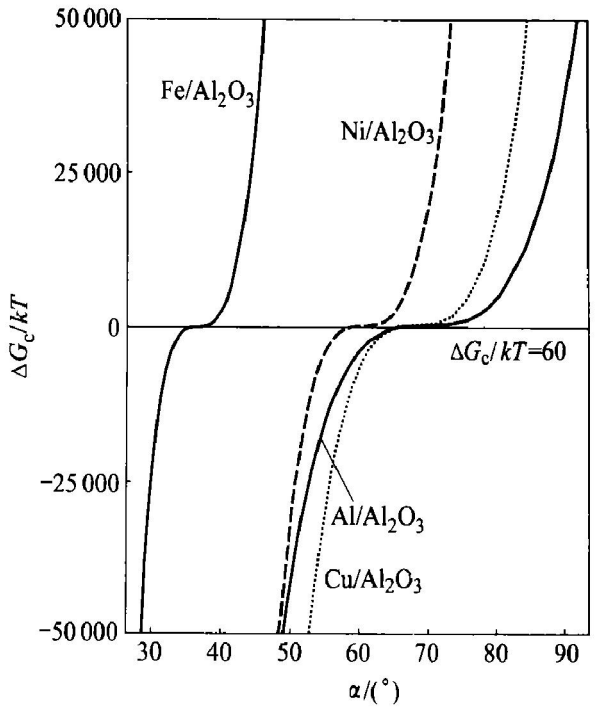

Fig. 5 Critical free energy for bubble nucleation versus apex angle of conical pit in alumina(Δp = 10 MPa)

the adhesion work calculated for different molten metals on alumina. It can be seen from Fig. 5 that the required critical apex angle (α) is about 93°, 90°, 78°, 41° in Al, Cu, Ni, Fe molten metals, respectively. For smaller than critical apex angles and deep enough pits, bubble nucleation will occur without the need to overcome an activation barrier. Such pits are thus extremely effective heterogeneous nucleation sites. In addition, the size of the critical apex angle also reflects the probability of bubble nucleation in a melt. So it can be seen from Fig. 5 that the probability of bubble nucleation progressively decreases from Al, Cu, Ni to Fe molten metal, which is resulted from the increasing adhesion work of liquid metal on alumina (see the data in Table 1). The much greater adhesion work of liquid metal on its solid ensures that pits in the solid metal would be effective as nucleation sites only if the apex angle is extremely small. So the possibility of bubble nucleation in conical pits in the solid metal is very small.

Most nonmetallic impurities are brittle and likely to contain microscopic cracks which may act as het-

erogeneous sites for nucleation. Polycrystalline metals will contain grain boundaries, which may be grooved. The nucleus geometry is taken to be a wedge out of a sphere, as shown in Fig. 6. If the bubbles nucleate in a V-shape crack of included angle α, the free energy in this case is

$$\Delta G = -\Delta p \frac{4}{3}\pi r^3 \frac{\alpha}{2\pi} + (\sigma_{sg} - \sigma_{ls})\pi r^2 + \sigma_{lg} 4\pi r^2 \frac{\alpha}{2\pi} \quad (8)$$

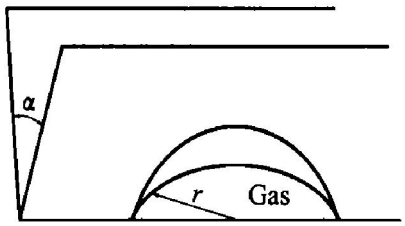

Fig. 6 Schematic drawing of bubble growing in wedge-shape crack

Very shallow cracks will be effective nucleation sites in that the required activation energy is very small. The corresponding free energy to form a critical radius of bubble is calculated from Eq. (9):

$$\Delta G_c = \frac{1}{3}\frac{[\pi W + \sigma_{lg}(2\alpha - \pi)]^3}{(\alpha \cdot \Delta p)^2} \quad (9)$$

Fig. 7 plots the critical nucleation energy vs the apex angles of the crack for physically reasonable materials. It can be seen from Fig. 7 that the required critical apex angle (α) is about 65°, 63°, 56°, 31° in Al, Cu, Ni, Fe molten metals, respectively. Most cracks are expected to have an apex angle smaller than 50° and are thus attractive heterogeneous nucleation sites for bubbles. The results also show that the probability of bubble nucleation progressively decreases from Al, Cu, Ni to Fe molten metal. With increasing W, the critical apex angle decreases. For nucleation at the solid metal interface, W is expected to be an order of magnitude higher. Accordingly, nucleation would occur only for extremely small values of α or under extremely high Δp. But this kind of situation is not possible under the conditions of GASAR processing.

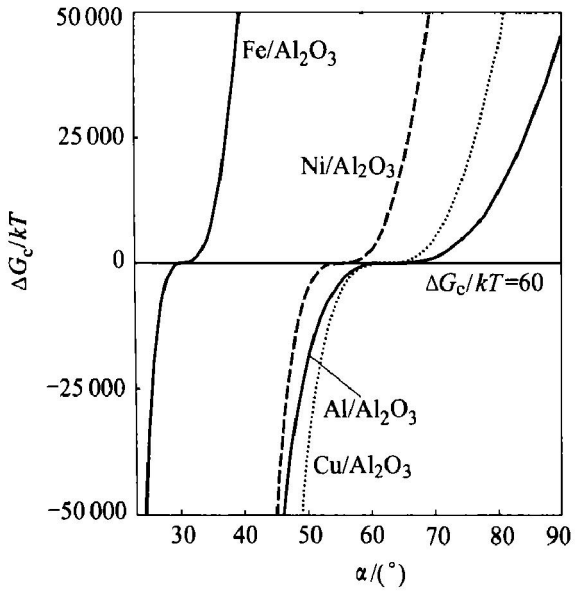

Fig. 7 Critical free energy for bubble nucleation versus apex angle of crack in alumina(Δp = 10 MPa)

3 CONCLUSIONS

1) Homogeneous nucleation of bubbles in the molten melt or the solidified region does not occur under the conditions of GASAR processing. The heterogeneous nucleation is the only feasible way.

2) The nucleation of bubbles as caps on the solid surface of impurities is not possible under the conditions of GASAR processing. Although the solidification front itself also can be a site for heterogeneous nucleation, the bubble nucleation is still ruled out due to a higher W of several Joules per square meter.

3) In the case that the bubble nucleation in a conical pit in alumina, the required critical apex angles (α) are about 93°, 90°, 78°, 41° in Al, Cu, Ni, Fe molten metals, respectively. In the case that the bubble nucleation in a crack in alumina, the required critical apex angles (α) are about 65°, 63°, 56°, 31° in Al, Cu, Ni, Fe molten metals, respectively. These conditions can be fulfilled easily. So this kind of heterogeneous nucleation is the most feasible way in GASAR process.

4) The probability of bubble nucleation progressively decreases from Al, Cu, Ni to Fe molten metal.

REFERENCES

[1] Walukas D M. GASAR Materials: A Novel Approach in the Fabrication of Porous Materials[M]. DMK TEK Inc, 1992.

[2] Shapovalov V I. Microstructural Design by Solidification Processing[M]. Lavernia E J, Gungor M N. The Minerals, Metals & Materials Society, 1992. 207-216.

[3] Sridhar S, Russell K C. Advances in Physical Metallurgy [M]. Amsterdam: Gordon and Breach Publishers, 1996. 315-324.

[4] Hirth J P, Pound G M. Condensation and Evaporation: Nucleation and Growth Kinetics[M]. Oxford: Pergamon Press, 1963. 149-161.

[5] Allen B C. Liquid Metals—Chem and Phys[M]. New York: Dekker, 1972. 161.

[6] Apprill J M, Poirier D R, Maguire M C. Gasar Porous metals process control[A]. Materials Research Society Symposium-Proceedings[C]. San Francisco, California: MRS, 1998. 291-296.

[7] Yamamura S, Shiota H, Murakami K, et al. Evaluation of porosity in porous copper fabricated by unidirectional solidification under pressurized hydrogen[J]. Mater Sci Eng, 2001, A318: 137-143.

[8] Bonenberger R J, Kee A J, Everett R K. Characterization of porous GASAR aluminum[A]. Materials Research Society Symposium-Proceedings[C]. San Francisco, Cal-

ifornia: MRS, 1998. 303 - 320.

[9] Pattnaik A, Sanday S C, Vold C L. Microstructure of Gasar porous copper ingots[A]. Materials Research Society Symposium-Proceedings[C]. San Francisco, California: MRS, 1995. 371 - 376.

[10] Fredriksson H, Svensson I. On the mechanism of pore formation in metals[J]. Metall Trans B, 1976, 7: 599 - 606.

[11] Tiwari S N, Beech J. Origin of gas bubbles in aluminum [J]. Metal Sci, 1978, 12: 356 - 362.

[12] Iwahori H, Yonekura K, Yamamoto Y, et al. Occurring behavior of porosity and feeding capabilities of sodium and strontium modified Al-Si alloys[J]. A F S Trans, 1990, 98: 167 - 173.

[13] Brondyke K J, Hess P D. Interpretation of vacuum gas test results for aluminum alloys[J]. AIME Trans, 1964, 230: 1542 - 1546.

[14] Laslaz G, Laty P. Gas porosity and metal cleanliness in aluminum casting alloys[J]. A F S Trans, 1991, 99: 83 - 90.

[15] Chidambaram P R, Edwards G R, Olson D L. A thermodynamic criterion to predict wettability at metal-alumina interfaces[J]. Metall Trans B, 1992, 23: 215 - 222.

(Edited by PENG Chao-qun)